Supplement of Biogeosciences, 21, 671–688, 2024
https://doi.org/10.5194/bg-21-671-2024-supplement

Biogeosciences Open Access EGU

Supplement of

Central Arctic Ocean surface–atmosphere exchange of CO_2 and CH_4 constrained by direct measurements

John Prytherch et al.

Correspondence to: John Prytherch (john.prytherch@misu.su.se)

1 pCO_2w and pCH_4w measurements

For both pCO_2w and pCH_4w, a merged dataset is created by averaging syringe and bottle measurements from the same location and similar times (sample times within 1 hour). Figure S2 shows all measurements prior to averaging.

Both syringe and bottle samples were analysed for pCH_4w using GC, but with differing methods as described in section 2.2. Syringe samples have consistently higher pCH_4w than bottle samples, with a mean difference of 5.64 ± 3.07 μatm. This difference could be due to sharp near surface gradient and the syringes sampling at a shallower depth (upper few cm) than the bottles (approximately 10 cm depth). This though would suggest a higher surface oversaturation. Furthermore, there is a similar disagreement between the bottle and syringe measurements during overside sampling, where water is sampled from a bucket within which any gradient is likely mixed out. The syringe-bottle difference could be due to accidental intake of ice into the bottle during sampling, lowering any measured dissolved gas concentration, but this was avoided where possible. The difference is likely from some other sampling bias between the two methods or error from the differing analyses performed on the samples.

For determination of surface pCO_2w, bottle samples were taken and analysed for DIC and TA, then pCO_2w was calculated using the CO2SYS toolbox as described in Section 2.2. The mean propagated uncertainty in computed pCO_2w was 27.1 ± 28.5 µatm based on the mean analytical uncertainties of the input pair DIC (5.0 µmol kg^{-1}) and TA (3.4 µmol kg^{-1}). The larger uncertainties are associated with low-salinity samples with low DIC and TA content (~50-120 µmol kg^{-1}). Considering the full range of analytical uncertainties of the input pair DIC (7.5 µmol kg^{-1}) and TA (5.9 µmol kg^{-1}) the mean propagated uncertainty in computed pCO_2w was 42.6 ± 45.0 µatm. Syringe samples were analysed for pCO_2w using GC in the same way as for CH_4 and as also described in Section 2.2. The difference in pCO_2w between the two methods was 51 ± 44 μatm which is similar to the upper levels of the estimated total uncertainty in pCO_2w derived from DIC and TA.

2 Freeze onset date

The local time of freeze-onset was determined from surface skin temperature measurements from the KT15 IR following the methods of Rigor et al. (2000) and Mortin et al. (2013) (Fig. S3). A threshold of either -1°C or -2°C is applied to the 14-day median filtered temperature. Using the -1°C threshold, the freeze onset occurs August 16. Temperatures increase noticeably after this date, and the -2°C threshold, which gives the freeze onset as August 25, appears to better represent the regime shift.

3. Eddy covariance gas flux measurements

Measurements of surface atmosphere CO_2 and CH_4 flux were also made throughout the expedition from an eddy covariance (EC) system installed on Oden's foremast. This system comprises a Metek uSonic-3 heated anemometer at mast top (20.3 m above mean sea level) alongside an inlet through which air is drawn down to a LGR Fast Greenhouse Gas Analyser, sampling at 10Hz. The airstream is dried using a Nafion drier prior to sampling. Transit time is approximately 5.6 seconds. Corrections are applied for platform motion, airflow distortion and high frequency signal loss and the corrections and system are described in more detail in Prytherch et al. (2017).

Post-cruise analysis of the EC system determined that fluxes in sea-ice regions were in general below the limit of detection of this system: An artificial time lag of 150 s was used to decorrelate the vertical wind and gas mixing ratio prior to flux calculation. The standard deviation of the resulting fluxes, shown in Fig. S4 below, gives a measure of the noise level in the system. Averaging of fluxes within a time window reduces the noise level, as per Dong et al., 2021b (Fig. S5), but the system remains too insensitive to measure the fluxes encountered during SAS. The noise levels determined here (CO_2 16 mmols m^{-2} day^{-1}; CH_4 52 μmol m^{-2} day^{-1}) provide an upper constraint on the magnitude of the surface-atmosphere fluxes during SAS. Noise levels here are higher than those determined from the same instrument at a land-based coastal station on the South Coast of the UK (Yang et al., 2016), presumably due to additional measurement noise from the large, moving measurement platform, and the harsh environment.

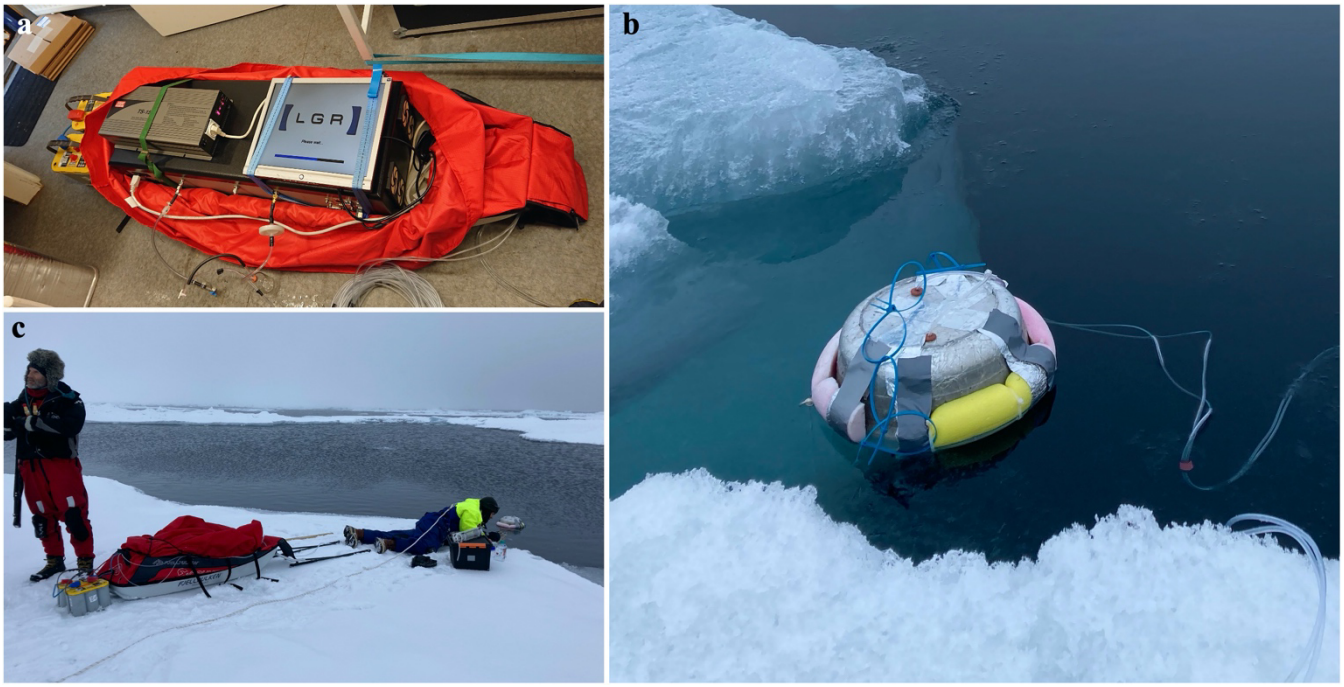

Figure S1. a) Chamber flux system consisting of an LGR Greenhouse Gas Analyser cavity enhanced laser spectrometer, power supply and tubing connections, mounted in a sled. b) Floating chamber during deployment in a sea-ice lead. c) Chamber flux system during ice-based deployment.

a)

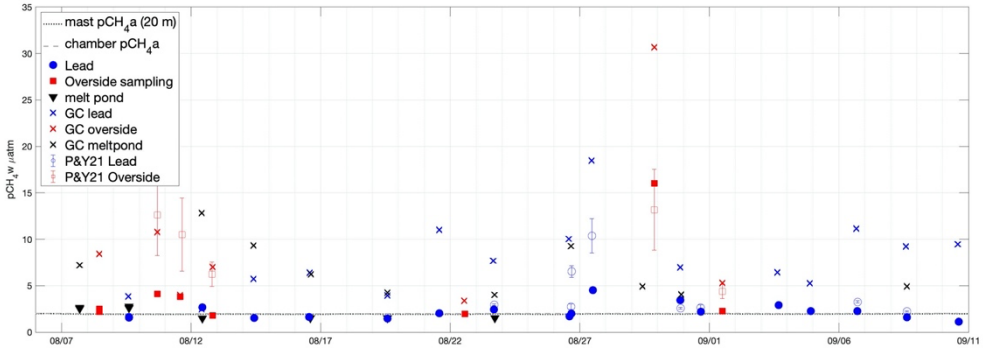

b)

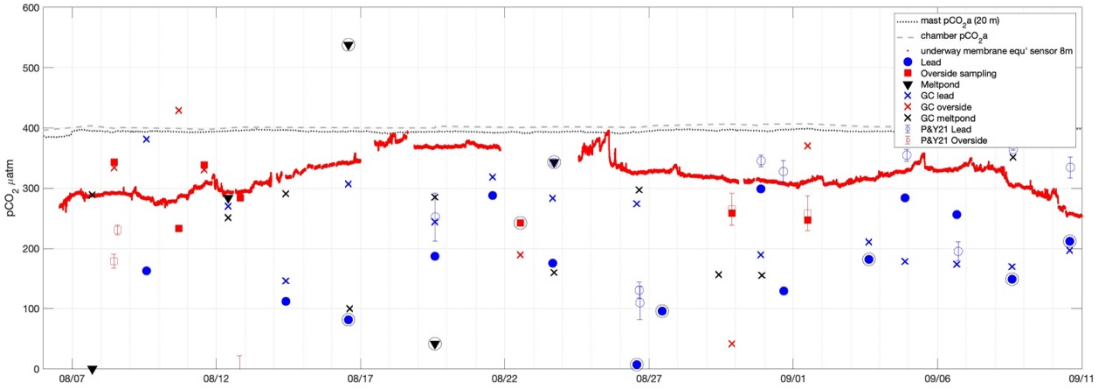

Figure S2. Time series of partial pressures of a) CH_4 and b) CO_2 in near-surface atmosphere and water during SAS2021. Solid markers show dissolved partial pressures determined from surface samples; outline markers show partial pressures determined using Eq. (1) and the parameterisation of Prytherch and Yelland (2021), excluding unphysical negative partial pressures. Colours indicate the location from which the sample was taken. 'GC' measurements, shown as crosses, refer to the syringe-based measurements.

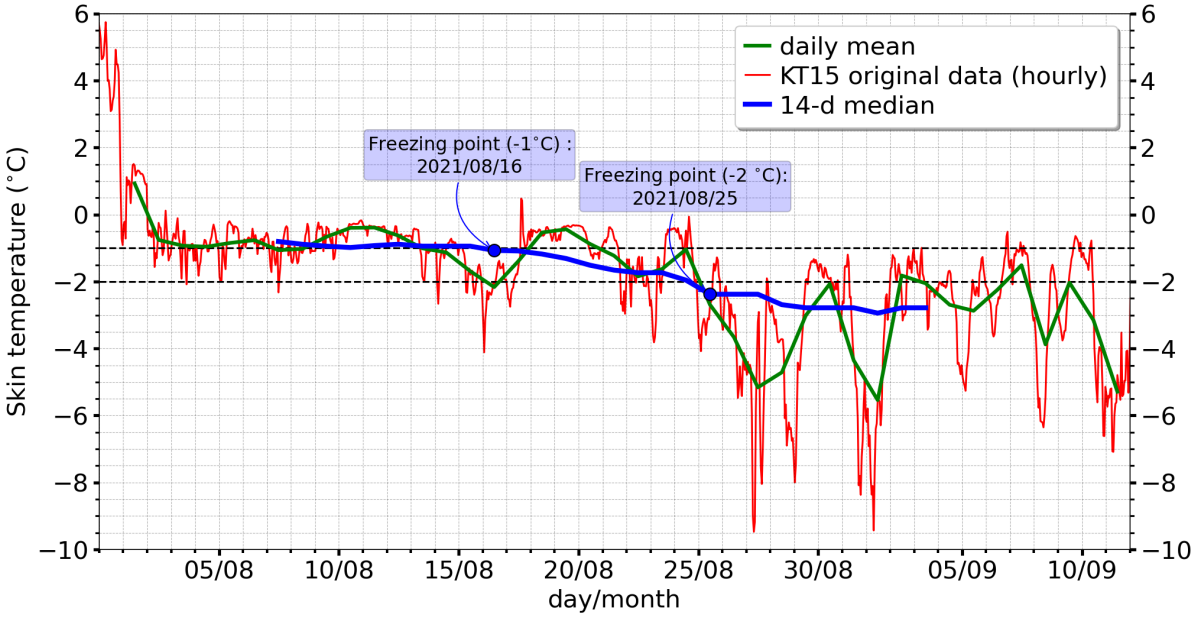

Figure S3. Surface temperature during SAS2021 measured with IR sensors onboard *Oden*, averaged to hourly and daily values, and with a 14-day running median.

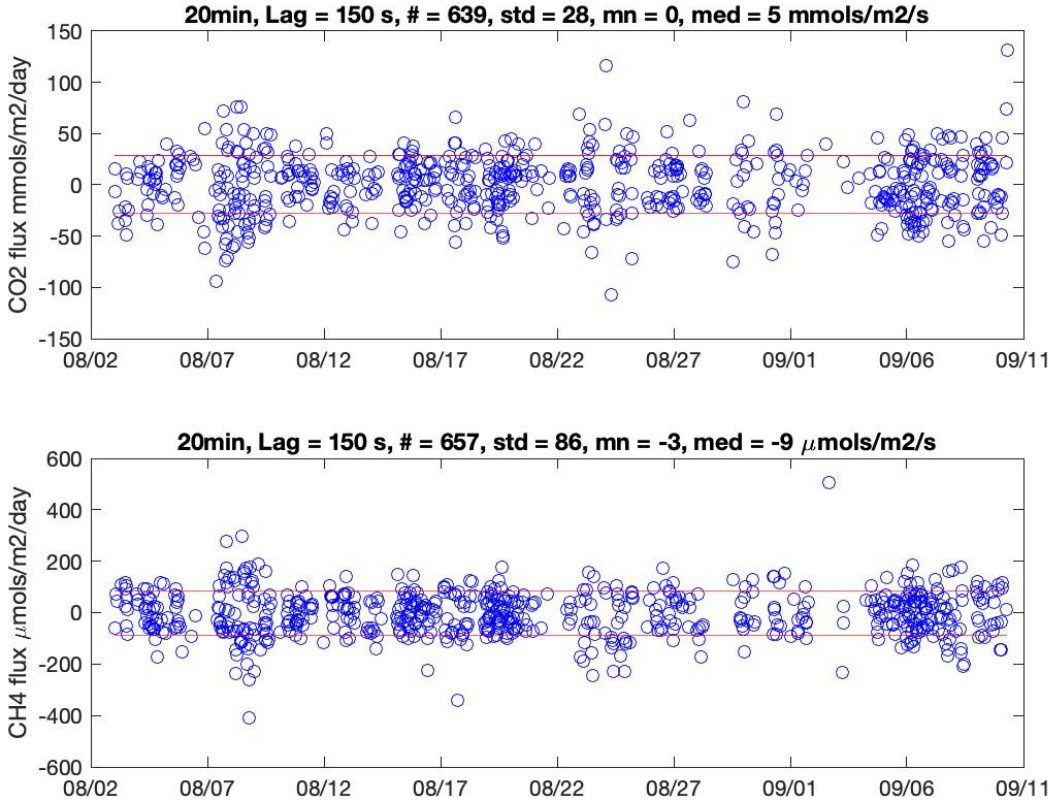

Figure S4. Noise level for the foremast cavity-enhanced spectrometer determined during SAS2021. Noise is determined by calculating 20-minute duration fluxes with a time lag of 150 s imposed on the spectrometer measurements relative to the vertical wind. The noise is then estimated as the standard deviation of these 'null' fluxes, shown as the horizontal lines.

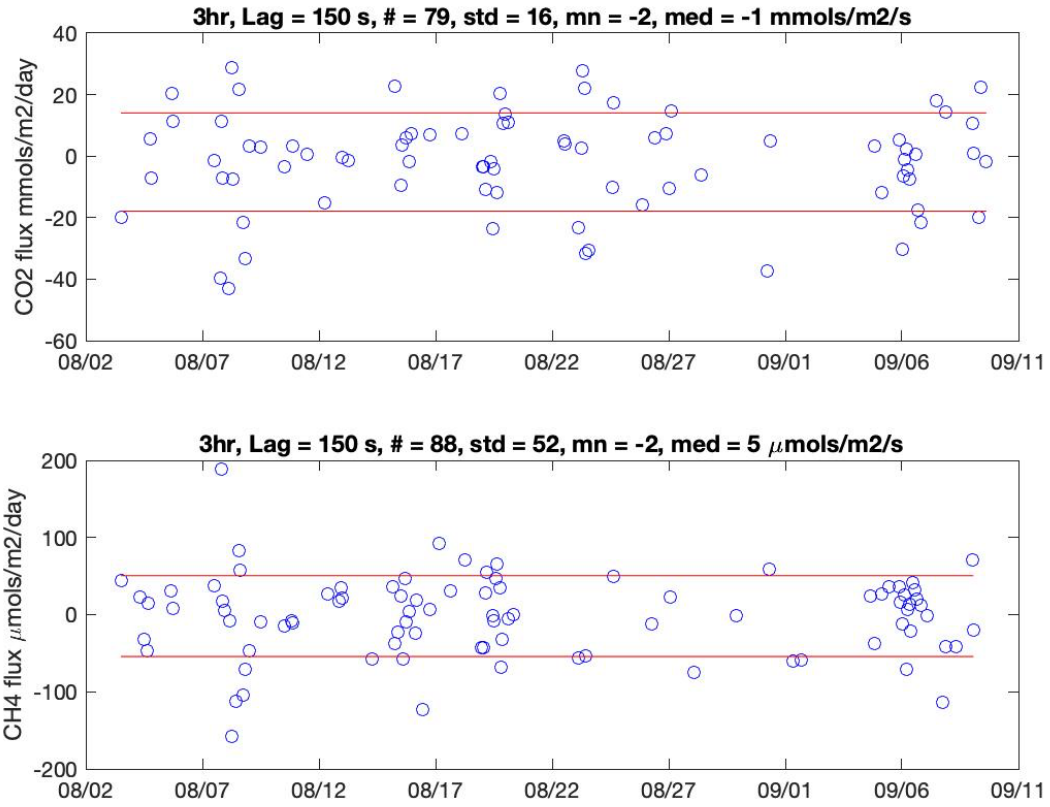

Figure S5. Noise level as per Fig. S4 determined for 3-hourly averages of the 20-minute fluxes.

70

Station	Lat °	Lon °	Date	T °C	S	U m s^{-1}	Width m	pCO_2w μatm	pCH_4w μatm	# samples	F_{CO2} mmol m^{-2} day^{-1}	F_{CH4} μmol m^{-2} day^{-1}
LGR ice-based												
9	89.92	67.5	8/16	-1.6	30.8	2.3	30	194 ± 113	4 ± 2.4	7	-2.7 ± 0.3	-
10	89.11	-150	8/19	-0.2	1.2	5	7.5	216 ± 29	2.7 ± 1.2	10	-6.2 ± 1.7	-
13	88.65	-129.3	8/23	-1.8	30.2	10.8	7.5	229 ± 54	5.1 ± 2.6	7	-6.6 ± 0.5	3.2 ± 0.3
14	87.86	-86.8	8/26	-1.2	28	5.5	12	141 ± 133	4.6 ± 4.2	6	-7.3 ± 0.4	0.6 ± 0.3
15	87.85	-86.7	8/26	-1.7	24.7	5.6	33	141 ± 133	4.6 ± 4.2	6	-7.1 ± 0.7	3.4 ± 0.5
16	87.83	-85.5	8/27	-1.6	28.8	3.7	33	163 ± 66	11.5 ± 7	6	-3.4 ± 0.4	1.6 ± 0.4
19	86.52	-57.3	8/30	-1.6	29.5	5.1	5	244 ± 55	5.2 ± 1.8	8	-2.5 ± 0.4	0.7 ± 0.1
20	86.49	-56.1	8/31	-1.7	29.7	6.9	5	129	2.2	5	-3.5 ± 0.8	0.9 ± 0.4
22	84.92	-33.5	9/3	-1.2	25.8	1.6	50	196 ± 14	4.7 ± 1.8	8	-4.8 ± 0.3	-
23	84.16	-32.3	9/4	-1.7	30.3	4	5	231 ± 53	3.8 ± 1.5	6	-1.5 ± 0.3	-
24	84.52	-24.5	9/6	-1.8	29.9	5.9	30	215 ± 41	6.7 ± 4.4	8	-6.6 ± 0.5	1.2 ± 0.1
25	83.86	-2.6	9/8	-1.3	20.4	7.3	1	160 ± 10	5.4 ± 3.8	8	-3.2 ± 0.1	0.6 ± 0.1
26	82.46	9.1	9/10	-1.9	32	8.2	1	204 ± 8	5.3 ± 4.2	8	-7.9 ± 1.9	-
Li7200 ice-based												
6	88.99	24.9	8/12	-1.8	30.1	6.5	80	270 ± 43	-	6	-6.7 ± 2.7	-
8	89.61	16.8	8/14	-0.9	15.8	1.6	30	129 ± 17	-	7	-4.1 ± 0.7	-
10	89.11	-150	8/19	-0.2	1.2	4.9	7.5	216± 29	-	8	-4.6 ± 0.6	-
11	88.74	-137.1	8/21	-1.6	29.8	3.5	5	303 ± 15	-	5	-2.7 ± 0.4	-
LGR overside												
2	86.39	32.1	8/8	-1.6	32.9	10.6	30	339 ± 5	4.4 ± 3.1	10	-20.7 ± 1.1	-
3	86.4	32.4	8/8	-1.7	32.8	11.6	10	339 ± 5	4.4 ± 3.1	6	-19.9 ± 0.9	-
4	88.04	29.5	8/10	-0.4	28.2	3.9	20	331± 98	7.4 ± 3.3	7	-19.1 ± 2.4	8.5 ± 3.5
5	88.49	28.9	8/11	-1.2	32.1	2.6	5	335 ± 4	3.9 ± 0.1	10	-12.6 ± 1.9	2.2 ± 1
7	88.95	23	8/12	-1.1	31.3	5.6	8	286 ± 2	4.4 ± 2.6	7	-15.6 ± 1.4	4.9 ± 1.5
12	88.52	-129.1	8/22	-1	23	1.8	5	216 ± 26	2.7 ± 0.7	9	-3.5 ± 0.5	-
18	87.34	-63.2	8/29	-1.6	29.7	5.1	10	150 ± 108	16	6	-6.7 ± 1.3	16.3 ± 6.3
21	86.28	-43.1	9/1	-1.9	29.8	4.1	10	309 ± 61	3.8 ± 1.5	8	-3.4 ± 0.7	1.7 ± 0.5

75 80 85 90 95 100

Table S1. Air-water flux measurements made with floating chamber systems, showing station number (as per Fig. 1) location and date, water surface temperature, salinity, 10 m wind speed, lead width, and dissolved gas partial pressures. Flux uncertainties are the standard error of the flux samples within each measurement period. Partial pressure uncertainties are the standard error of the averaged surface measurements.

Lat °	Lon °	Date	T °C	Floe z m	Snow z m	Freeboard m	# samples	F_{CO2} mmol m^{-2} day^{-1}
86.30	30.6	8/7	0.2	1.8	0.05	-	4	-2.9 ± 1.2
87.05	31.2	8/9	0.4	1.2	0.05	-	5	-0.1 ± 0.1
88.99	24.9	8/12	0.2	2.5	0.05	-	4	-2.2 ± 1.3
89.61	16.8	8/14	0.0	1.3	0.08	0.16	4	0.2 ± 0.2
89.11	-150.0	8/19	0.0	1.6	0.12	0.29	2	0
88.74	-137.1	8/21	0.1	3	0.1	0.4	2	-2.9
88.65	-129.4	8/23	0.0	1.6	0.09	0.15	2	-0.6
87.86	-86.8	8/26	-1.6	2.4	0.08	0.19	3	0
86.52	-57.3	8/30	-1.1	2.0	0.09	0.23	2	0
86.49	-56.1	8/31	-	1.4	0.09	-	3	-1.6 ± 0.3
84.93	-33.5	9/3	-0.0	2.4	0.08	0.19	3	-0.7 ± 0.4
84.16	-32.3	9/4	-2.6	1.6	0.1	0.18	3	-2.8 ± 1.5
84.52	-24.5	9/6	-0.4	2.1	0.12	0.2	3	-0.7 ± 0.3
83.86	-2.6	9/8	-2.6	2.2	0.08	0.34	3	-1.2 ± 0.6

Table S2. Air-snow chamber flux measurements made with the EGM-4 chamber flux system, surface (snow) temperature, floe depth, snow depth and freeboard.